5

Advanced SnO_2-Based Ceramics: Synthesis, Structure, Properties

Mihaiu Maria Susana, Scarlat Oana,
Zuca Stefania and Zaharescu Maria
"Ilie Murgulesc" Institute of Physical Chemsitry of the Romanian Academy
Romania

1. Introduction

Tin dioxide presents specific optical and electrical properties and a good chemical stability which confers special characteristics to the SnO_2 based materials.
SnO_2 belongs to the important class of transparent conductor oxide materials that combine low electrical resistance with high optical transparency in the visible range of the electromagnetic spectrum. These properties are requiered for optoelectronic applications i.g light emitting diodes, electrode materials in solar cells flat panel displays, transparent field effect transistors[Wagner, 2003; Presley et al., 2004]. Tin dioxide is aslo an oxidation catalyst and its activity and selectivity can be substantially improved by incorporation of various additives [Mihaiu et al., 2002]. Another field in which tin dioxide plays a dominant role is in solid state gas sensors. A wide variety of oxides exhibit sensitivity towards oxidizing and reducing gases by a variation of their electrical properties, but SnO_2 was one of the first considered, and still is the most frequently used, material for these applications [Caldararu et al., 1999]. The sensor properties of SnO_2 depend not only on such factors as the oxide's surface stoichiometry, the methodology used to prepare the powder, temperature and atmosphere of calcination but also, and mainly, on the high specific area deriving from the low densification of this oxide. Nowadays, SnO_2 is certainly one of the main polycrystalline ceramic candidates to compete with the traditional multicomponent ZnO-based varistors (voltage-dependent resistor-VDR's), especially because of high electrical stability and its more simple microstructure [Bueno et al., 2007]. High density in polycrystalline ceramics is essential for high varistor properties, since the phenomena involved for good varistor properties occur in the region of the material's grain boundaries. The main restriction in a wider use of this type of material is related to poor sintering ability of the SnO_2-based compositions. This behaviour is related to the low diffusivity of the SnO_2 structure and predominance of the nondensifying mechanisms (surface diffusion and evaporation-condensation). The latter result in grain and pore growth, thus limiting the final density [Varela et al., 1990]. The sintering problem is further complicated by the formation of deleterious intermediate phases above 1273K and high vapor pressurre of SnO [Dolet et al., 1992]. Dense SnO_2-based materials have been obtained either by using sintering additives (e.g.,CuO) to promote densification by liguid-phase mechanism or by applying high pressures (e.g., in hot isostatic pressing technique).

In recent years, aluminium smelters have made great progress in reducing emissions of various gaseous and particulate compounds that may have a negative impact on the global, regional and local environment [Popescu et al., 2007]. The selection of a suitable anode material has proved to be very difficult task. It should be resistant to evolving oxygen and cryolite-alumina melt at ~ 950° C , i.e., in the melt, which is used as solvent for oxides. The maximum allowable wear rate for a commercial use is evaluated as 1.0 cm/year at a current density of 0.8 A/cm^2. The electric conductivity and electrocatalytic activity with respect to oxygen evolution should be high enough to prevent extra losses of electricity. The material should be resistant to mechanical and thermal stress, and its components should not be poisonous for the raw aluminum, to avoid further purification. The only materials that meet these requirements are a number of oxides. Over the years, many materials have been tested on a laboratory scale with mixed success. One such material is tin oxide (SnO_2) doped with different additives which is considered to be a promising material for manufacturing electrodes for melts electrolysis due to their excellent corrosion resistance and heat resistant properties. Studies on the electrical conductivity of SnO_2-based ceramic materials revealed the major influence exerted by the nature of the dopants and the thermal treatment, i.e. the sintering conditions. The electrical resistance is claimed [Zuca et al.,1999] to be decreased drastically (by 4 to 5 orders of magnitude) by the addition of Sb_20_3 as, following its limited solubility in the SnO_2 lattice, the concentration of charge carriers increases. On the other hand, the sintering capacity was found to be greatly improved by the addition of CuO [Dolet et al., 1995]. Although a list of various potential additives has been suggested by Varela, their influence on the sintering properties (namely densification) and electrical conductivity has not been systematically investigated so far [Varela et.al., 1992]. The influence of a series of oxide additives (individual and various combinations), namely Sb_2O_3, CuO, ZnO, Fe_2O_3, Cr_2O_3, TiO_2, MnO_2 and MoO_3 on the sintering capacity and electrical conductivity of the SnO_2-based ceramic materials has been investigated. From among various oxide additives tested, only CuO was found to promote the densification of the composite. The addition of Sb_2O_3, which is claimed to increase the electrical conductivity, is only effective in the presence of CuO addition [Zuca et al., 1991].

During the electrochemical investigations some irregularities were found (it seemed that a small amount of oxygen was consumed on the anode). To understand the causes of these phenomena in order to diminish or remove them it is considered necessary to investigate the chemical processes between the three oxides (SnO_2, Sb_2O_3, and CuO) that take place during the thermal treatment of their mixture.

In this work we propose a review of chemical processes that occur in the SnO_2- Sb_2O_3- CuO system over the whole concentration range of the components. The obtaininig of the sintered materials by conventional ceramic method and spark plasma sintering and the electriacal behaviour of the oxide materials belonging to this system is also approached.

2. Phase formation in the SnO_2-Sb_2O_3-CuO ternary system

A summary of physical characteristics of individual SnO_2, Sb_2O_3, and CuO compound is given in the Table 1.

Based on the experimental data determined under non-isothermal conditions up to 1773K for pure components [Zaharescu et al., 1991], the following has been established:

1. no effects were observed for SnO_2 in the 293-1773 K temperature range;

2. the endothermal reduction of CuO to Cu_2O which starts at 1348 K, is followed by eutectic melting of the two copper oxides;
3. the oxidation of Sb_20_3 to Sb_2O_4, which takes place within a wide temperature interval from 713 to 933 K is accompanied by a well marked exothermal effect and a mass increase; the endothermal effect observed at 1433 K indicates the vaporization of Sb_2O_4.

Physical and structural characteristics	SnO_2	Sb_2O_3	Sb_2O_4	CuO
Mineral	cassiterite	valentinite	cervantite	tenorite
Culour	white	colorless	white	black
Molecular weight	150,69	291,50	307,50	78,54
Symmetry	tetragonal	romboedric	orthorhombic	monoclinic
Space group	D_{4h}^{14} (P4/mnm)	V_h^{10} (P_{ccn})	*Pna*21	C_{dh}^{6C}(c2/c)
Lattice parameters (Å)	$a_0=b_0=4,7374$ $c_0=3,1864$	$a_{0=}$ 4,92 b_0=12, 46 c_0= 5,42	a = 5.43 b = 4.79 c = 11.73	$_{0=}$ 4,92 b_0=12, 46 c_0= 5,42 β =99°29′
Ionic radius (Å)	Sn^{4+}= 0,71		Sb^{3+} =0,76 Sb^{5+} =0,62	Cu^{2+}=0,72
Density (g/cm^3)	6,95	5,67	6.64	6,3- 6,49
Melting point (K)	-O;1800;>2200*		1433 sublimes	1599
Boiling point (K)	2073 sublimes			2273
Refraction index	2⊥ c 2,11// c	2,18 2,35 2,35	2,00	2,63

Table 1. Physical and structural characteristics of SnO_2, Sb_2O_3, CuO [Wyckoff, 1963, 1964]

2.1 Solid state reactions in the component subsystems

2.1.1 SnO_2-CuO binary system

The experimental data on the SnO_2-CuO binary system have been published in several papers [Zaharescu et al., 1991; Scarlat et al., 1999]. The thermal analysis of (1-x)SnO_{2-x}CuO compositions, in non-isothermal conditions, in air, up to 1773 K, underlined that the thermal effects registrated could be assigned exclusively to the presence of CuO in the reaction mixture. The reduction process of CuO to Cu_2O over 1273 K as well as the formation over 1373 K of the liquid phase have been evidenced. No binary compounds were formed.

The results obtained by isothermal treatments at 1173, 1273 and 1473 K of the (1-x)SnO_{2-x}CuO mixtures were also analyzed. Thus, for the samples with 1-10% content of CuO only SnO_2 was identified by X-ray diffraction, no matter of treatment temperature. Although the

ionic radii of the two ions are close (0.71 Å for the Sn^{4+} and 0.72 Å for the Cu^{2+}) due to their different structures and especially their different valence, the formation of a a solid solution between the two oxides is unlikely to occur. The disappearance of characteristic diffraction lines of copper oxide and the sharp contraction of these samples was assigned to its penetration into the liquid phase (eutectic melt), which facilitates rapid rearrangement of the ions [Zaharescu et al., 1991; Dolet et al., 1992]. It was observed that in isothermal condition the reaction of CuO reduction, namely: $CuO \rightarrow Cu_2O$ takes place at substantially lower temperature compared with the non-isothermal measurements. The phase composition of the binary mixtures with a content of CuO >30%, thermally treated at 1273 K consists in a mixture of SnO_2, CuO and Cu_2O. The samples with a CuO content exceeding 10% fused when thermally treated at 1473 K. The shrinkage of the tested samples increased with increasing temperature while the porosity decreased; at 1273 and 1473 K samples with a zero porosity were obtained, apparently owing to the presence of the liquid phase.
As a conclusions, at temperature over 1273 K the SnO_2-CuO initial binary system transforms into the SnO_2- CuO- Cu_2O pseudo-ternary system. In the presence of CuO the sintering ability of SnO_2 is promoted. Below 1173 K, the rate of densification can be explained in terms of viscous flow model [Zaharescu et al.,1993], while at higher temperature a copper-rich liquid is formed and rearrangement is occuring even for short sintering time.

2.1.2 SnO_2-Sb_2O_3 binary system

Widely used as catalysts in catalytic oxidation reactions, the oxide powders belonging to the SnO_2-Sb_2O_3 system are studied by many research groups in this field [Harrison et al., 1999;. Park et al., 1999] especially in the subsolidus domain.
In accordance with the rules of formation of substitional solid solutions (the sizes of two ions differ by less than 15%, have similar valency factor, chemical affinity and structure type) tin dioxide can form a limited solid solution with antimony oxides. Solid solubility limit depends on the method of preparation and treatment temperature. Volta obtained monophasic powders with rutile type structure by coprecipitation of tin (IV) and antimony (V) chlorides and heat treatment at 773 for 16 hours [Volta et al., 1985] of the resulted hidroxides. Similar results have been obtained by Vlasova for the powders with the antimony content of 40% and thermal treatment at 873 K temperature[Vlasova et al.,1990]. At 1273 K the amount of antimony atoms in solid solution decreases to 30% and at 1473 K to 4%. Orel et al. have found that regardless of the initial concentration of antimony, the maximum amount of Sb_2O_4 entered into the SnO_2 lattice is of 2.38 mol at 1473 K [Orel et al., 1995]. The interactions that occur between the two oxides in the whole concentration range in non isothermal (up to 1773 K) and isothermal conditions at 873, 1073, 1273 and 1473 K temperatures were investigated in paper [Zaharescu et al., 1991]. The temperature interval of the exothermal effect corresponding to the oxidation of Sb_2O_3 to Sb_2O_4 is substantially narrowed in the binary mixtures (695-716 K) compared to the pure Sb_2O_3 (713-933 K) which suggests the catalysing effect of SnO_2 in the oxidation process. It may be also assumed that in the reaction with SnO_2, antimony participates as a heterovalent mixture of the $Sb(III)Sb(V)O_4$ type. The endothermal effect observed at high Sb_20_3 concentrations at temperatures above 1423 K which is accompanied by a mass loss, is assigned to the vaporization of Sb_2O_4. The exothermal effect indicates the oxidation of Sb_2O_3 to Sb_2O_4 at 873 K however, the latter oxide has not been identified by X-ray diffraction at concentrations up to 10% (all concentrations are given in mass %). This can be apparently assigned to the

formation of the solid solution owing to the substitution of antimony for tin in the SnO_2 crystal structure. Although the samples with a higher Sb_2O_4 concentration undergo deformation and peeling at higher temperatures which make them unsuited for the subsequent measurements. The concentration of Sb_2O_4 (up to 30%) in the solid solution apparently increases with increasing temperature (up 1273 K) and only SnO_2 is identified in the undeformed samples. The XRD results indicate the displacement of the pure SnO_2 diffraction peaks due to the formation of this rutile type of solid solution. All peaks were slightly shifted to the right after the solid solution was formed (larger angle or smaller both *a* and *c* lattice paramaters) with respect to pure SnO_2.
Taking into account that Sb_2O_3 in the presence of SnO_2 over 773 K in air, completly turns into Sb_2O_4 and the oxidation state of tin ions do not change, the question is what form of antimony ions enter the tin dioxide lattice. Vlasova proposed the following "formula" [Vlasova et al., 1990]:

(a) $Sn^{4+}_{1-2x}Sb^{3+}_{x}Sb^{5+}_{x}O^{2-}_{2}$ (b) $Sn^{4+}_{1-2x}Sn^{3+}_{x}Sb^{5+}_{x}O^{2-}_{2}$; (c) $Sn^{4+}_{1-x}Sb^{5+}_{x}e_xO^{2-}_{2}$;

(d) $Sn^{4+}_{1-5x}Sb^{5+}_{4x}V^{0}_{kx}O^{2-}_{2}$ (e) $Sn^{4+}_{1-x}Sb^{3+}_{x}O^{2-}_{2-x}V_{ax}$; (f) $Sn^{4+}_{1-x}Sb^{3+}_{x}O^{2-}_{2-x/2}V_{ax/2}$;

(g) $Sn^{4+}_{1-3x}Sn^{2+}_{x}Sb^{5+}O^{2-}_{2}$;

where e_x = free electrons
and V_k and V_a cation and anion vacancies, respectively
When contents of antimony atoms do not excede 3% in the SnO_2 latice, the following "compounds" were identified by EPR: $Sn^{4+}_{1-x}Sb^{3+}_{x}O^{2-}_{2-x}V_{ax}$; $Sn^{4+}_{1-x}Sb^{5+}_{x}e_xO^{2-}_{2}$;

$$Sn^{4+}_{1-2x}Sn^{3+}_{x}Sb^{5+}_{x}O^{2-}_{2}.$$

In the case of higher concentration of antimony embeded in the SnO_2 lattice the most likely the resulted solid solution has the the following composition: $Sn^{4+}_{1-2x}Sb^{3+}_{x}Sb^{5+}_{x}O^{2-}_{2}$. By EXAFS it has been established that Sb dopants occupy Sn sites in the rutile structure [Chadwick et al.,1993; Rockenberger et al., 2000]. XANES measurements showed that the largest fraction of Sb has a valency of 5^+, although 3^+ was also observed in nanocrystalline SnO_2. The Sb^{3+} species may be due to a strong tendency of Sb to segregate to the surface [Dusastre et al., 1998; Slater et al., 1999].

2.1.3 Sb_2O_3-CuO binary system

Sb_2O_3-CuO binary system is the most complex subsystems of the SnO_2-Sb_2O_3-CuO ternary system. In this system, the formation of $CuSb_2O_6$ binary compound with pentavalent antimony has been reported. The compound has a tri-rutile structure, short-range and long range magnetic ordering. Under some special conditions, two other binary compounds, having a higher copper content, have been prepared: $Cu_4SbO_{4,5}$ and $Cu_9Sb_2O_{19}$ [Bystrom et al.,1944; Shimada et al.,1982; 1985;1988].Stan et al., have studied the (10-n)CuO + nSb_2O_3mol (n=0;1;….10) mixtures belonging to the Sb_2O_3-CuO binary system at room temperature. According to the thermal analysis results, the following solid state reactions occur [Stan et al.,1998] :

$$\approx 773\ K \quad Sb_2O_3 + 1/2\ O_2 = Sb_2O_4 \tag{1}$$

$$>1023\ K \quad Sb_2O_4 + CuO + 1/2\ O_2 = CuSb_2O_6 \tag{2}$$

$$>1223\ K\ \ CuSb_2O_6+7CuO=(1-r)\ CuSb_2O_6+7(1-r)CuO+\ 2rCu_4SbO_{4.5}+2rO_2 \qquad (3)$$

Where $r\epsilon\ (0,1)$ is the fraction of $CuSb_2O_6$ that transforms into $Cu_4SbO_{4.5}$.

In order to emphasize an intermediate stage in the compound formation, Fig. 1 shows the relative intensities of the X-ray characteristic lines for the mixtures thermally treated for only one hour.

The same compounds have been obtained in both isothermal treatment (one hour and three hours) and non-isothermal conditions. This points to the high reactivity of the oxides in this system. There is no evidence of $Cu_9Sb_2O_{19}$ compound formation. This compound as reported only for high pressures (see Table 2). Then, in the range of 293-1273 K at normal atmospheric pressure, the following compounds can be found in equilibrium: CuO, Cu_2O, Sb_2O_3, Sb_2O_4, $CuSb_2O_6$ and $Cu_4SbO_{4.5}$.

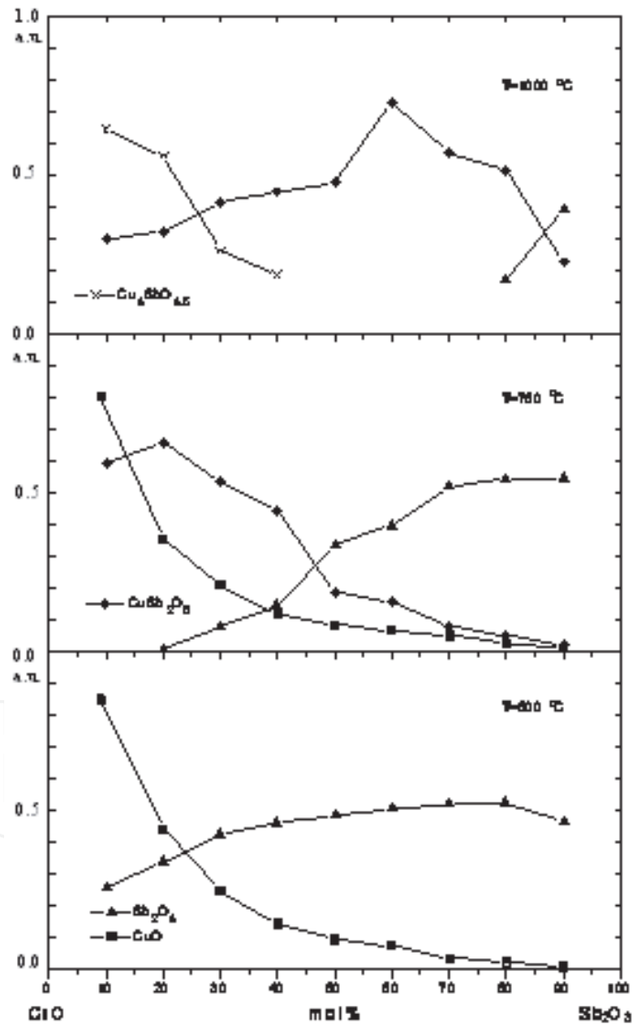

Fig. 1. Relative intensities of the X-ray characteristics lines for the binary mixtures thetmally treated at 773, 823 and 1273 K, one hour

All the experimental evidences show that equations (1), (2) and (3) are suficient to describe the reactions occuring in the Sb_2O_3-CuO binary system with increasing temperature. If the

reactions are considered as completed, including r=1 in equation (3), then the quatity of oxygen that is gained or lost can be calculated for each sample.
The atomic composition modifications during the thermal treatments for the four representative samples is given Fig.2. At room temperature the compositions lay on the Sb_2O_3-CuO line as shown in Fig.2. The composition line moves to Sb_2O_4-CuO at 773 K and changes to Sb_2O_4-$CuSb_2O_6$-CuO over 823 K. Finally, if the reaction (3) is completed at 1273 K, the compositions lay on the CuO- $Cu_4SbO_{4.5}$-$CuSb_2O_6$ - Sb_2O_4 .

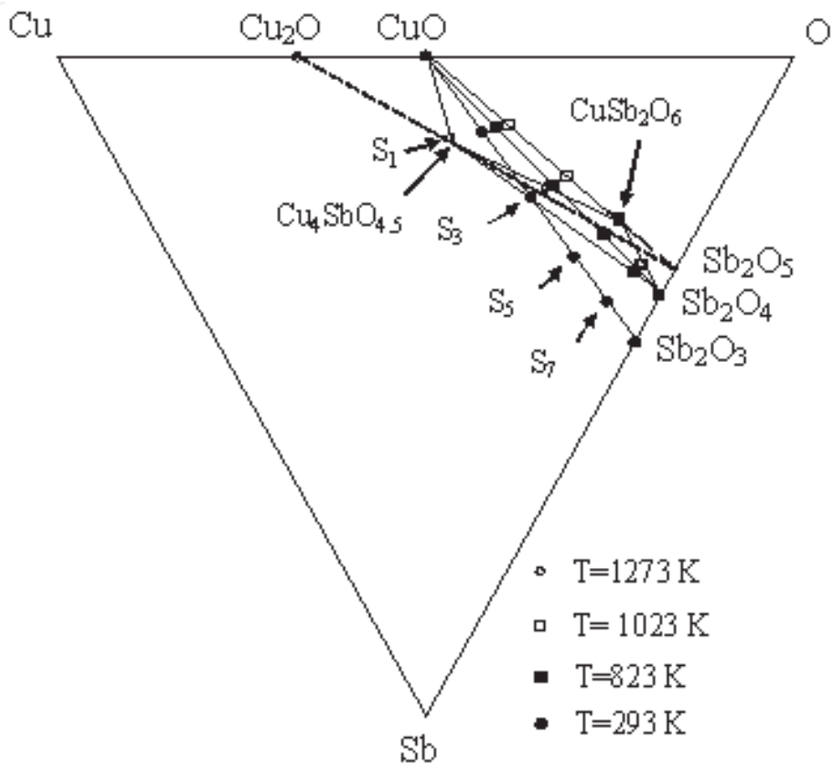

Fig. 2. Atomic compositions after the thermal treatment for the following initial mixtures: S_1 the mixture of 90 mol% of CuO and 10% mol of Sb_2O_3; S_3 the mixture of 70 mol% of CuO and 30% mol of Sb_2O_3; S_5 the mixture of 50 mol% of CuO and 50% mol of Sb_2O_3; S_7 the mixture of 30 mol% of CuO and 70% mol of Sb_2O_3 [Stan et al.,1998]

2.2 Solid state reactions in the SnO_2-Sb_2O_3-CuO ternary system

The SnO_2-Sb_2O_3-CuO ternary system have been investigated in the whole concentrations range isothermal and non-isothermal conditions in[Zaharescu et al.,1991;1993; Mihaiu et al.,1995] .In the Fig.3 experimental ternary compositions are graphically presented.
Equimolecular mixture of CuO and Sb_2O_3 (which leads to $CuSb_2O_6$ formation) determine the next evolution of the mixtures in the system and this ratio affords the classification of sample in three categories:
(I) CuO:Sb_2O_3=1 and the samples lie on SnO_2-equimolecular mixture;
(II) CuO:Sb_2O_3 >1 and the samples are belonging to the CuO-CuO.Sb_2O_3–SnO_2 pseudo-ternary system;

(III) $CuO:Sb_2O_3<1$ and the samples are belonging to the Sb_3O_3-$CuO.Sb_2O_3$–SnO_2 pseudo-ternary system [Zaharescu et al., 1993]

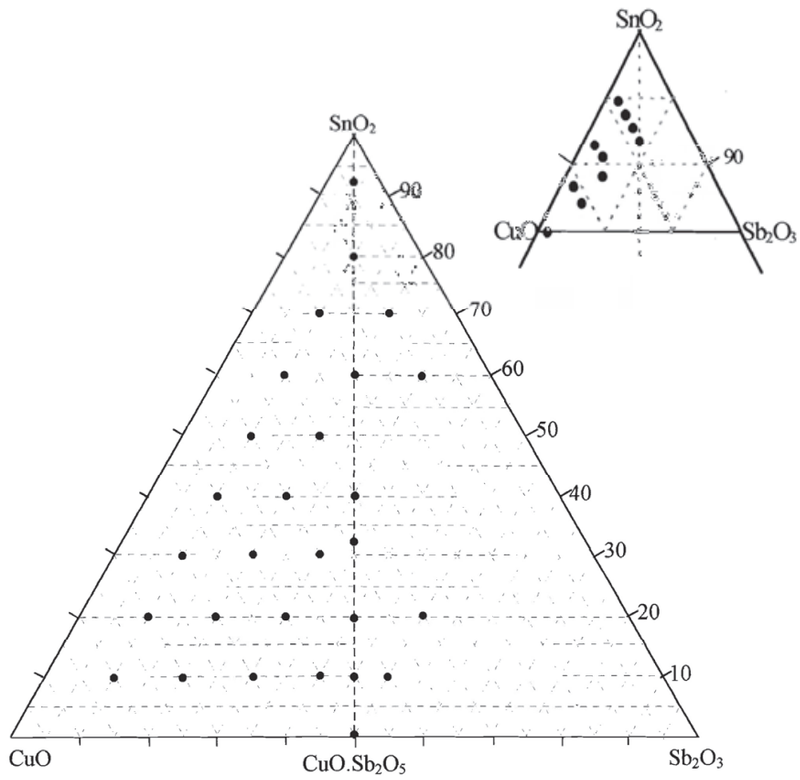

Fig. 3. Domain of the studied compositions in the SnO_2-Sb_2O_3 – CuO system [Zaharescu et al., 1999]

The oxidation of Sb_2O_3 to Sb_2O_4 (and Sb_2O_5), as well as the high temperature interactions of Sb_2O_3 with SnO_2 and respectively with CuO have been discussed in the section 2.1.1 and 2.1.3. The thermal behaviour of Sb_2O_3 in the presence of both mentioned oxides in non-isothermal conditions (up to 1273 K) is summarized in the Table 2 .For the mixtures from (I) categorie ($CuO:Sb_2O_3=1$) on can note that the oxidation of Sb_2O_3 to Sb_2O_5 is total and take place in two steps. The experimental weight increase is in good agreement with the theoretical one. The resulted phase composition of the samples corresponds to a mixture of SnO_2 and $CuSb_2O_6$. Accordigly, in the presence of both SnO_2 and CuO there is a higher tendency of Sb_2O_3 to react with CuO than to form solid solution with SnO_2.

In the ternary mixtures of molar ratio $CuO:Sb_2O_3>1$, a total oxidation of Sb_2O_3 to Sb_2O_5 is obtained; above 1233 K; a weight loss is also observed which is assigned to the reduction of CuO to Cu_2O. After thermal treatment the phase composition consists in SnO_2, $CuSb_2O_6$ and $Cu_4SbO_{4.5}$ mixtures.

In the ternary mixtures of molar ratio $CuO:Sb_2O_3<1$, in the first step Sb_2O_3 entirely oxidize to Sb_2O_4. In the second step the transformation of Sb_2O_4 to Sb_2O_5 is limited to the quantity required by $CuSb_2O_6$ formation.The unreacted Sb_2O_4 dissolves partially into SnO_2 with the formation of a solid solution with SnO_2 crystal structure.

Oxide compositions (%mol.)			Thermal effects (K)		Mass variation (%)		Assignment	Phase composition
SnO_2	Sb_2O_3	CuO	Endo	Exo	Exp.	Calc.		
93	3	4		695,728	+0.34	+0.34	[O] $Sb_2O_3 \longrightarrow Sb_2O_4$	SnO_2
80	10	10		713,733	+0.86	+1.01	[O] $Sb_2O_3 \longrightarrow Sb_2O_4$	SnO_2, $CuSb_2O_6$
					+0.47	+1.00	[O] $Sb_2O_4 \longrightarrow Sb_2O_5$	
70	10	20		713	+0.96	+1.06	[O] $Sb_2O_3 \longrightarrow Sb_2O_4$	SnO_2, $CuSb_2O_6$, $Cu_4SbO_{4.5}$
				1053	+0.96	+1.05	[O] $Sb_2O_4 \longrightarrow Sb_2O_5$	
			1233		-0.41	-0.52	$CuO \longrightarrow Cu_2O$ [-O]	
70	20	10		733	+1.65	+1.86	[O] $Sb_2O_3 \longrightarrow Sb_2O_4$	SnO_{2ss}, Sb_2O_4 $CuSb_2O_6$
					+0.76	+0.92	[O] $Sb_2O_4 \longrightarrow Sb_2O_5$	
60	20	20		748	+1.66	+1.94	[O] $Sb_2O_3 \longrightarrow Sb_2O_4$	SnO_2, $CuSb_2O_6$
				1073	+1.63	+1.91	[O] $Sb_2O_4 \longrightarrow Sb_2O_5$	
33.3	33.3	33.3		761	+3.07	+3.07	[O] $Sb_2O_3 \longrightarrow Sb_2O_4$	SnO_2, $CuSb_2O_6$
				1112	+2.90	+2.89	[O] $Sb_2O_4 \longrightarrow Sb_2O_5$	
10	45	45		713	+3.14	+3.96	[O] $Sb_2O_3 \longrightarrow Sb_2O_4$	$CuSb_2O_6$, SnO_2
				1148	+3.14	+3.89	[O] $Sb_2O_4 \longrightarrow Sb_2O_5$	
10	40	50		713,793	+3.44	+3.73	[O] $Sb_2O_3 \longrightarrow Sb_2O_4$	$CuSb_2O_6$, SnO_2, Cu_4SbO_4.
				1063	+3.55	+3.59	[O] $Sb_2O_4 \longrightarrow Sb_2O_5$	
			1223		-0.30	-0.43	$CuO \longrightarrow Cu_2O$ [-O]	
10	50	40			+3.98	+4.15	[O] $Sb_2O_3 \longrightarrow Sb_2O_4$	$CuSb_2O_6$, SnO_2, Sb_2O_4
					+3.12	+3.18	[O] $Sb_2O_4 \longrightarrow Sb_2O_5$	

Table 2. The results of differential thermal analysis and thermogravimetry of the ternary mixtures

The phase composition consists in SnO_{2ss}, Sb_2O_4, $CuSb_2O_6$ mixtures. In isothermal conditions the ternary mixtures have been themally treated at 873, 1073, 1273, 1373 and 1473 K. Samples thermally treated at lower temperatures (873,1073,1273 K) showed no linear

shrinkage but linear dilatation and high porosity pointing out an inadequate sintering [Zaharescu et al., 1999]. Besides oxide composition in Table 3 the phase components and the ceramic characteristics of studied mixtures thermally trated at 1373 K are given. In the categorie (I) ($CuO:Sb_2O_3$=1) the solid solutions with SnO_2 crystal structure (rutile) includes $CuSb_2O_6$ (tri-rutile structure) up to a limit of about 50 mol%. Below this limit a mixture of SnO_2 and $CuSb_2O_6$ is detected. A similar behaviour has been reported by Kikuchi in the SnO_2–MSb_2O_6 system (M=Zn,Mg) [Kikuchi et al., 1983]. As claimed by the author, $ZnSb_2O_6$ is solved in SnO_2 up to 50 mol% as $Zn_{1/3}Sb_{2/3}O_2$ at 1473K whereas SnO_2 is dissolved in $ZnSb_2O_6$ up to 20 mol% at the same temperature. The lattice parameters decreasd with decreasing SnO_2 contents. Similarly, $MgSb_2O_6$ dissolved in SnO_2 up to 50 mol% at 1523 K but SnO_2 was sparingly solved into $MgSb_2O_6$. In the categorie (II) ($CuO: Sb_2O_3$ >1) the same type of solid solubility has been observed. The compounds $CuSb_2O_6$ and $Cu_4SbO_{4.5}$ have been also identified by XRD for a large range of concentrations. For the mixture containing 10 mol% SnO_2, this compound was not identified. On can assume that SnO_2 dissolves in $CuSb_2O_6$ forming a solid solutin with tri-rutile structure. In the categorie (III) ($CuO: Sb_2O_3$<1) SnO_2-based solid solution and $CuSb_2O_6$ compound have been observed. Although in this system Sb_2O_3 is exceeding the necessary amont required by $CuSb_2O_6$ stoichiometry, it was not identified by XRD. This result suggests that the unreacted Sb_2O_4 dissolves preferentially in SnO_2 and hinders the dissolutions of $CuSb_2O_6$ in the SnO_2 crystal network.

Based on the experimental data, the authors [Stan et al.1997]reported that in SnO_2-Sb_2O_3-CuO ternary system besides the solid state reactions represented by 1-3 equations (section 2.1.3.), at temperature above 1273 K, the following reactions take place:

$$T > 1273\ K: \quad SnO_2 + CuSb_2O_6 \longrightarrow SnO_2(ss) \tag{4}$$

$$T > 1273\ K: \quad SnO_2 + CuSb_2O_6 + Sb_2O_4 \longrightarrow SnO_2(ss) \tag{5}$$

$$T > 1273\ K: \quad CuSb_2O_6 + SnO_2 \longrightarrow CuSb_2O_6(ss) \tag{6}$$

Evolution of the phase composition ofn the SnO_2-Sb_2O_3-CuO ternay system with thermal treatment at 873, 1073, 1273, 1373 K could be better visualized in a guaternary representation (Figure 4).

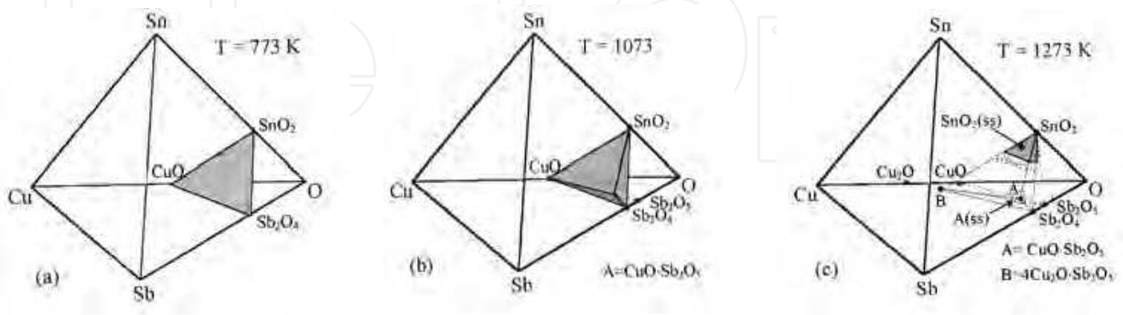

Fig. 4. Evolution of phase composition with thermal treatment temperature

In these representations the experimental ternary mixtures belonging to SnO_2-Sb_2O_4-CuO ternary subsystem at 773K, SnO_2-Sb_2O_4-CuO-$CuSb_2O_6$ pseudo-quaternary system at 1073 K andSnO_2-Sb_2O_4-$CuSb_2O_6$-$Cu_4SbO_{4.5}$ pseudo-quaternary system at temperatures >1273 K.

Crt. No.	Composition (mol.%)			Phase composition	Shrinkage %	Porosity %	Density g/cm^3
	SnO_2	Sb_2O_3	CuO				
(I) CuO: Sb_2O_3 =1							
1.	80	10	10	SnO_2(ss)	10	-	5.815
2.	60	20	20	SnO_2(ss)	10	0.16	5.9237
3.	40	30	30	SnO_2+ $CuSb_2O_6$	2	3.56	
4.	33.3	33.3	33.3	SnO_2+ $CuSb_2O_6$	+5	6.25	
5.	20	40	40	$CuSb_2O_6$ + SnO_2	+1	4.92	
(II) CuO: Sb_2O_3 >1							
1.	70	10	20	SnO_2(ss)	12	0.73	
2.	60	10	30	SnO_2(ss)+ $Cu_4SbO_{4.5}$	12	0.77	
3.	50	10	40	SnO_2(ss)+ $Cu_4SbO_{4.5}$	15	0.79	
4.	50	20	30	SnO_2(ss)+ $Cu_4SbO_{4.5}$	13	0.35	
5.	40	10	50	SnO_2(ss)+ $Cu_4SbO_{4.5}$	20	0.43	6.3018
6.	40	20	40	SnO_2(ss)+ $Cu_4SbO_{4.5}$	12	0.38	
7.	30	10	60	SnO_2(ss)+ $Cu_4SbO_{4.5}$	12	0.58	
8.	30	20	50	$CuSb_2O_6$ + SnO_2+ $Cu_4SbO_{4.5}$	9	0.33	5.9820
9.	30	30	40	$CuSb_2O_6$ + SnO_2+ $Cu_4SbO_{4.5}$	6	0.92	
10.	20	10	70	$CuSb_2O_6$(ss) + $Cu_4SbO_{4.5}$	11	0.31	5.8785
11.	20	20	60	$CuSb_2O_6$ (ss)+ $Cu_4SbO_{4.5}$	6	0.11	6.0248
12.	20	30	50	$CuSb_2O_6$(ss) + $Cu_4SbO_{4.5}$	7	0	5.6297
13.	10	10	80	$Cu_4SbO_{4.5}$ + SnO_2(ss)	12	1.45	
14.	10	20	70	$CuSb_2O_6$(ss) + $Cu_4SbO_{4.5}$	10	0	5.8088
15.	10	30	60	$CuSb_2O_6$(ss) + $Cu_4SbO_{4.5}$	7	0	5.7790
16.	10	40	50	$CuSb_2O_6$(ss)	+5	5.29	
(III) (CuO: Sb_2O_3<1							
1.	70	20	10	SnO_2(ss)	1		
2.	60	30	10	SnO_2(ss) + $CuSb_2O_6$	+2		
3.	20	50	30	$CuSb_2O_6$ + SnO_2(ss)	+3		
4.	10	50	40	$CuSb_2O_6$(ss)	-		

Table 3. Oxide composition, phase composition, ceramic characteristics of the ternary mixtures thermally treated at 1373 K, 1 h

2.2.1 SnO_2–$CuSb_2O_6$ binary system

In the subsolidus domain, the formation of the $CuSb_2O_6$ binary compound was found to be a basic stage in the SnO_2-Sb_2O_3-CuO ternary sistem evolution and, consenquently, SnO_2–$CuSb_2O_6$ binary system was considered to be representative for the study of Sn-Sb-Cu-O quaternary system. In the work [Scarlat et.al., .2002], the high temperature interactions between SnO_2 and $CuSb_2O_6$ have been investigated both in non-isothermal and isothermal conditions. The experimental compositions are expressed as (1-x)SnO_2-x $CuSb_2O_6$, with x= 0, 0.025, 0.04, 0.06, 0.08, 0.1, 0.2, 0.25, ….0.75, 0.8…1, covering the whole concentration range. The thermal treatments in the non-isothermal conditions pointed out that more than one chemical process developed between 1398 – 1723 K which are exclusively a result of the presence in the initial mixture of $CuSb_2O_6$ (see Table 2, section 2.1.3.) according to the following equations:

$$T \approx 1476\ K: \quad 4\ CuSb_2O_6 \longrightarrow Cu_4SbO_{4.5} + 7/2\ Sb_2O_3 + 9/2O_2 \tag{7}$$

$$T \approx 1520\ K: \quad 2\ Cu_4SbO_{4.5} \longrightarrow 4\ Cu_2O + Sb_2O_3 + O_2 \tag{8}$$

This observation suggests that no solid state interactions have occurred between SnO_2 and $CuSb_2O_6$ in non-isothermal conditions.

The isothermal treatements of the binary mixtures at 1273 K (one, three and ten hours) and at 1373 and 1473 K respectively (three hours) have been done. An increase of the temperature value over 1473 K was not possible due to reactions (7) and (8), resulting in the decomposition and partial melting of pure $CuSb_2O_6$ and solid solutions.

Based on the experimental results, the subsolidus phase relations of SnO_2–$CuSb_2O_6$ system are presented in Fig.5.

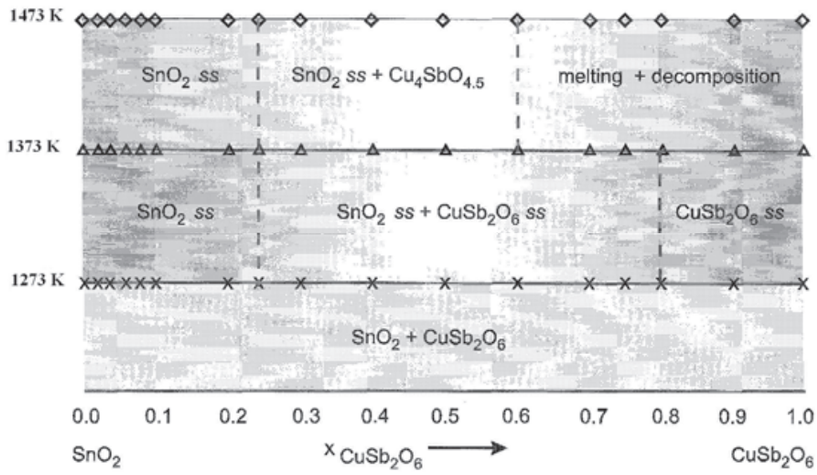

Fig. 5. Subsolidus phase relations in the SnO_2 –$CuSb_2O_6$ system

Accordingly, the system was divided at 1373 K into the following three subsolidus domain:

$$0 < x \leq 0.25 \longrightarrow SnO_{2\,ss} \text{ described as } Sn_{1-x}Cu_{x/3}\,Sb_{2x/3}O_2$$

$$0.25 < x < 0.8 \longrightarrow SnO_{2\,ss} + CuSb_2O_{6\,ss}$$

$$0.8 < x \leq 1 \longrightarrow CuSb_2O_{6\,ss} \text{ described as } Cu_{1-x}Sb_{2(1-x)}Sn_{3x}O_6$$

Due to the $CuSb_2O_6$ decomposition and to the presence of the liquid phase extending from the Cu-O system [Scarlat et al.,20020], the phase relationships establishing becomes more difficult over 1473 K.
One has established that SnO_2–$CuSb_2O_6$ is a pseudobinary system with solid solubility limit of the end members.

2.2.2 Solid state solutions

The results previously presented evidenced the formation of large domains of unique phase with rutile as well as tri-rutile structure. The mechanism of their formation was approached in the papers [Mihaiu et al., 1995; Scarlat et al., 2002]. It considers framing the initial ternary mixtures from which the unique phase is formed in the subsystems component of the Sn-Sb-Cu-O quaternary system: (1) SnO_2–$CuO.Sb_2O_5$ pseudobinary system (the ratio $CuO:Sb_2O_3$ =1), (2) SnO_2–$CuO.Sb_2O_5$-CuO pseudoternary subsystem (the ratio CuO: $Sb_2O_3 \geq 1$) and (3) SnO_2 –$CuO.Sb_2O_5$-Sb_2O pseudoternary subsystem (the ratio CuO: $Sb_2O_3 \leq 1$). As has been stated previously, in all cases the formation of the $CuSb_2O_6$ binary compound, which precedes the formation of the SnO_2 solid solution as unique phase, was found to be a basic stage in the interactions at high temperature of the initial components.
In the following, the formation of solid solutions from the ternary mixtures belonging to the SnO_2-Sb_2O_3-CuO system as well as from the SnO_2 and $CuSb_2O_6$ binary mixtures will be presented. The rutile type solid solution unique phase was formed from the ternary mixtures with a SnO_2 molar content of over 70% and a ratio $CuO:Sb_2O_3 \geq 1$, and was thermally treated at 1273K for 3 h. The lattice parameters calculated from X-ray diffraction data decrease due to the inclusion of $CuSb_2O_6$ in the SnO_2 lattice [Mihaiu et al., 1995]. The solid solution which was formed is of $Sn^{4+}_{1-x}Cu^{2+}_{x/3}Sb^{5+}_{2x/3}O_2$ ($0<x<1/2$) type .The excess of copper oxide forms with SnO_2 a liquid phase which is responsible for the sample densification at 1273K. In case of the ternary mixtures with the ratio CuO: $Sb_2O_3 \leq 1$ (molar content of $SnO_2 \geq 70\%$) the formation of the rutile type solid solution as a unique phase takes place in two steps. In the first step, Sb_2O_4 dissolves in the SnO_2 lattice (1273 K), and in the second step $CuSb_2O_6$ is included in the SnO_2 lattice (1273K). The decrease of the parameters is more important than previously mentioned [Mihaiu et al., 1995].
The following formula was proposed: $Sn^{4+}_{1-x}Cu^{2+}_{x/5}Sb^{3+}_{x/5}Sb^{5+}_{3x/5}O_2$, in which $0<x<1/2$
In case of the ternary mixtures with the ratio CuO: Sb_2O_3 =1, the unique phase of rutile type solid solution was obtained up to the composition domain with over 60 mol% SnO_2.
The development of phase composition of the ternary mixture with 60 mol% of SnO_2, 20 mol% of Sb_2O_3 and 20mol% of CuO at different temperature is presented in the Fig.6. [Zaharescu et al., 2001] At 1373 K temperature only SnO_{2ss} solid solution with $Sn_{0.5}Cu_{0.17}Sb_{0.33}O_2$ formula should be observed. To clarify the way $CuSb_2O_6$ is dissolved into SnO_2 lattice to form a solid solution, IR absoption spectra (Fig.7) for the same samples utilized to identify by XRD the formation of SnO_2- based solid solution were recorded.
One can draw the following conclusions:
After thermal treatment, one hour at 873 K the presence of SnO_2 by the 635 cm^{-1} strongest band was identified. One can assume that CuO bands overlap those of SnO_2, whose presence is predicted from the shoulder located at 580 cm^{-1}.The bands group that comes up at 735, 480 and 377 cm^{-1} may be assigned to the presence of α- Sb_2O_4. At 1073 K the SnO_2 typical band (650 cm^{-1}) does not change its position but becomes less clear. The bands of α-Sb_2O_4 come out less outlined in the same wave number domain as at 873 K. The authors

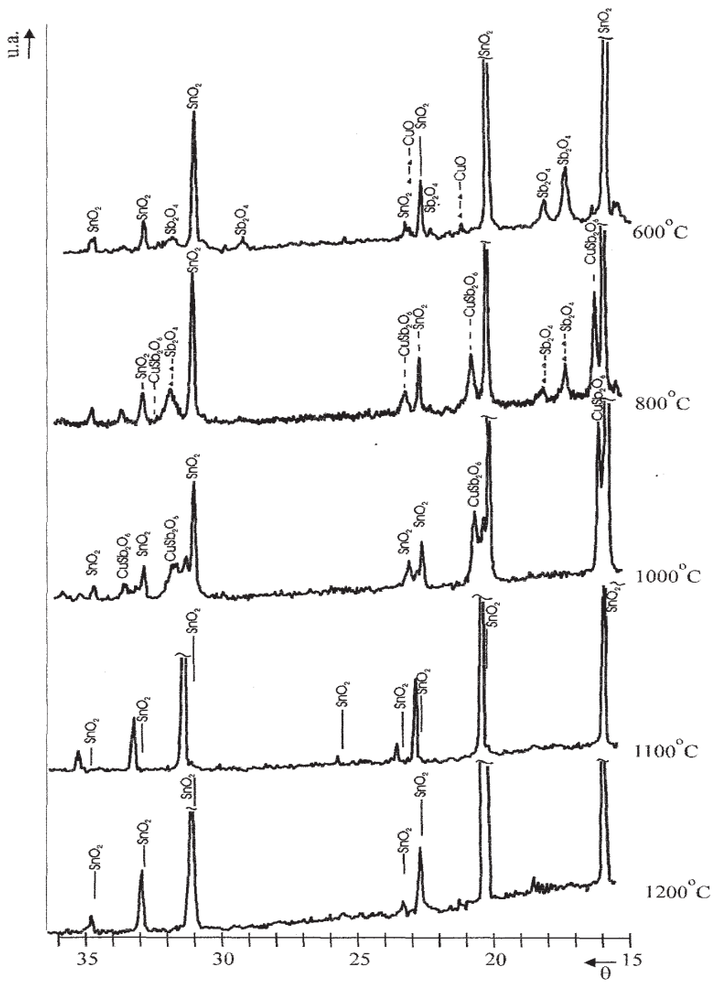

Fig. 6. XRD patterns of the mixture with initial composition: 60mol% of SnO_2, 20 mol% of Sb_2O_3 and 20 mol% of CuO, thermally treated one hour at 873, 1073,1273,1373 and 1473 K.

noted the presence of two extra-bands (located at 575 cm^{-1} and 815 cm^{-1}) and a shoulder at 680 cm^{-1} assigned to $CuSb_2O_6$ presence whose formation started at about 1023K. At 1273 K the SnO_2- based solid solution besides SnO_2 and $CuSb_2O_6$ presence was identified by X-ray diffraction. IR measurements have shown an intensity decrease for the SnO_2 strongest absoption band and its splitting into 682 cm^{-1} and 630 cm^{-1} bands. At this temperature better conditions are offered to $CuSb_2O_6$ formation which can be noticed from its typical bands (575 cm^{-1} and 815 cm^{-1}) those bands intensify and an extra-band at 680 cm^{-1} appears. At >1273 K the typical pure oxides and $CuSb_2O_6$ compound bands disppear and one can note an abnormal decrease of transmission, assigned to the dissolution of $CuSb_2O_6$ into the SnO_2 lattice.

The typical IR bands disappearance of the SnO_2- based solid solution may be explained by the strong interaction between the lattice phonons and a higher charge carrier concentration determined by the solid solution formation. The assumption is sustained by semimetallic behaviour of the sample [Ionescu et al., 1997].

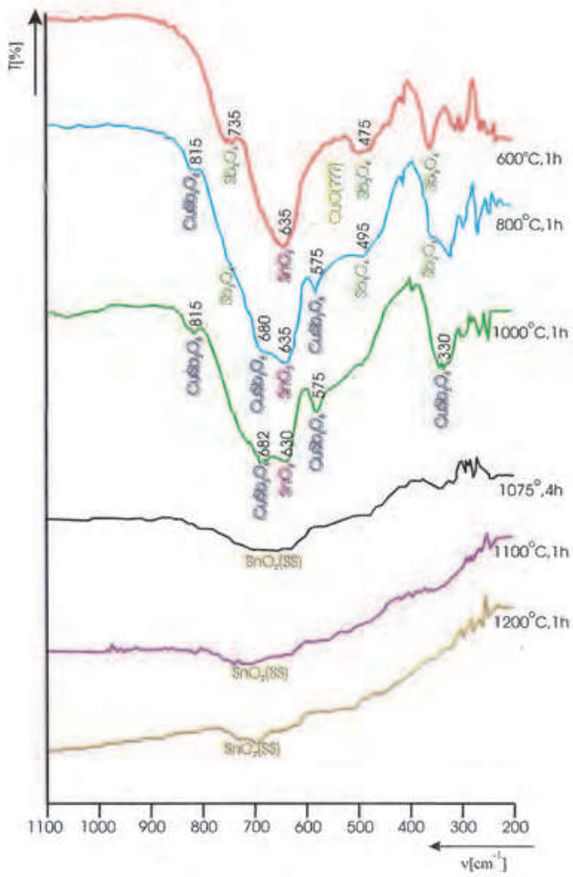

Fig. 7. IR Spectra of the mixture with initial composition:60 mol% of SnO_2, 20 mol% of Sb_2O_3 and 20 mol% of CuO, thermally treated one hour at 873, 1073,1273,1343,1373 and 1473 K

The scanning electron micrograph(SEM) of the $Sn_{0.5}Cu_{0.17}Sb_{0.33}O_2$ solid solution thermally treated at 1373 K (Fig.8) show homogeneous textures with mono-sized grains. No vitreous phase is noticed. According with the results of the chemical microanalysis obtained from SEM a good agreement between initial composition of the mixture and $Sn_{0.5}Cu_{0.17}Sb_{0.33}O_2$ (SS) should be observed.

Tri-rutil type solid solutions occurr at concentration below 20 mol% of SnO_2 at 1273. The cell parameters calculated from the diffraction data show a small variation of the elementary cell as compared to those of $CuSb_2O_6$.

In the papers following [Mihaiu et al., 1999; 2001; Scarlat et al., 2002] the formation of *rutil* (SnO_2) and *tri-rutil* type ($CuSb_2O_6$) solid solutions was studied starting not with the three component oxides (SnO_2, Sb_2O_3, CuO) but with SnO_2 and $CuSb_2O_6$ thermally treated at la 1373 K, 3 hours.

The lattice parameters for $SnO_{2\,ss}$ and $CuSb_2O_6$ ss were calculated from diffraction data.

For the tin rich-end members of the series, which crystallise with the *rutile* type lattice, the measured a_o [Å] and c_o [Å] lattice parameters obey Vegard's Rule:

$$a_o = 4.736 - 0.0016 \cdot x_{CuSb2O6} \pm 0.002 \text{ Å}$$

$$c_o = 3.1865 + 0.016 \cdot x_{CuSb2O6} \pm 0.002 \text{ Å}$$

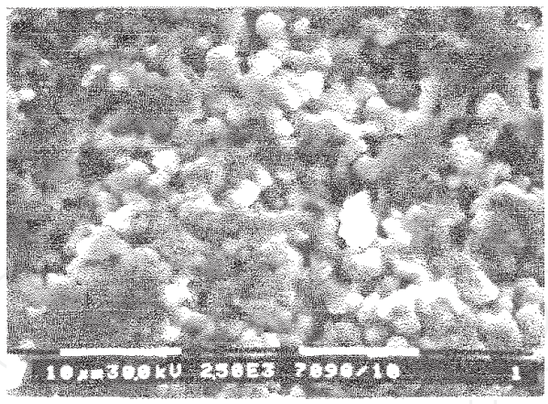

The chemical microanalysis from Scanning electron micrographs (SEM) data for the $Sn_{0.5}Cu_{0.17}Sb_{0.33}O_2$ solid solution thermally treated at 1373 K:

% at.	Exp.	Calc.
Sn	18.23	16.67
Cu	6.77	5.55
Sb	11.11	

Fig. 8. SEM image of the $Sn_{0.5}Cu_{0.17}Sb_{0.33}O_2$ solid solution thermally treated at 1373 K

The solid solubility limit of $CuSb_2O_6$ in SnO_2 was estimated to be at $x_{CuSb2O6}$ = 0.25, in accordance with previous results obtained using the mixture with 60mol% of SnO_2, 20 mol% of Sb_2O_3 and 20 mol% of CuO .The variation of the lattice parameters for the composition which consists from SnO_{2ss} is shown in Fig. 1(a, b)

For the SnO_2 based solid solutions (Fig. 9), a linear decrease of the lattice parameters a and c was noticed up to a 25% mol. CuSb2O6 content in the initial mixture. At higher amount of $CuSb_2O_6$ in the mixture, the lattice parameters remain constant, confirming the assumption that the dissolution of $CuSb_2O_6$ in the SnO_2 matrix take place until half of the Sn^{4+} were substituted with Cu^{2+} and Sb^{5+} in the 1:2 ratio.

In this way the composition of the higher limit of the solid solution formed corresponds to the $Sn_{1/2}Cu_{1/6}Sb_{2/3}O_2$ compound (the same value as when starting with individual tin, antimony, copper oxides). In the case of the sample which contains the highest quantity of $CuSb_2O_6$ incorporated in the SnO_2 matrix, the magnetic susceptibility ($\chi_{g,293K}$) value of $2.5 \times 10^{-6} cm^3/g$ is very close to those obtained in the case of mixture of phases ($\chi_{g,293K} = 2.9\times 10^{-6} cm^3/g$). That could be a confirmation of the inclusion of the $CuSb_2O_6$ compound in the rutile type structure as a $Cu_{1/3}Sb_{2/3}O_{6/3}$ moiety [Mihaiu et al., 2001].

The $CuSb_2O_6$ based solid solutions were lesser studied [Mihaiu et al., 2001; Scarlat et al., 2002]. It is known that $CuSb_2O_6$ compound crystallizes in a distorted monoclinic trirutile structure in space group $P2_{1/c}$ or $P2_{1/n}$ [2] with folllowing unit cell parameters: a=4.6324Å, b=4.6359 Å, c=9.2967 Å and β°=91.12. The trirutile type structure can be generated from the rutile structure by tripling the c-axis due to the chemical ordering of the divalent and pentavalent cations. The structure consists of a network of edge and corner sharing CuO6 and SbO6 octahedra. The Cu^{2+} and Sb^{5+} cation position are such that the magnetic Cu^{2+} ions are separated from each other by two sheets of diamagnetic ions. In fact, the magnetic cation sublattice is the same as that of the K_2NiF_4 structure, which is the canonical example of a square lattice two-two-dimensional antiferomagnet. Nakua established that $CuSb_2O_6$ compound shows the clearest evidence for the dominance of one-dimensional correlations

in the short range ordered regime with the magnetic susceptibility value $\chi_{g,293K}$=3,7.10^{-6}cm3/g [Nakua et al., 1991].

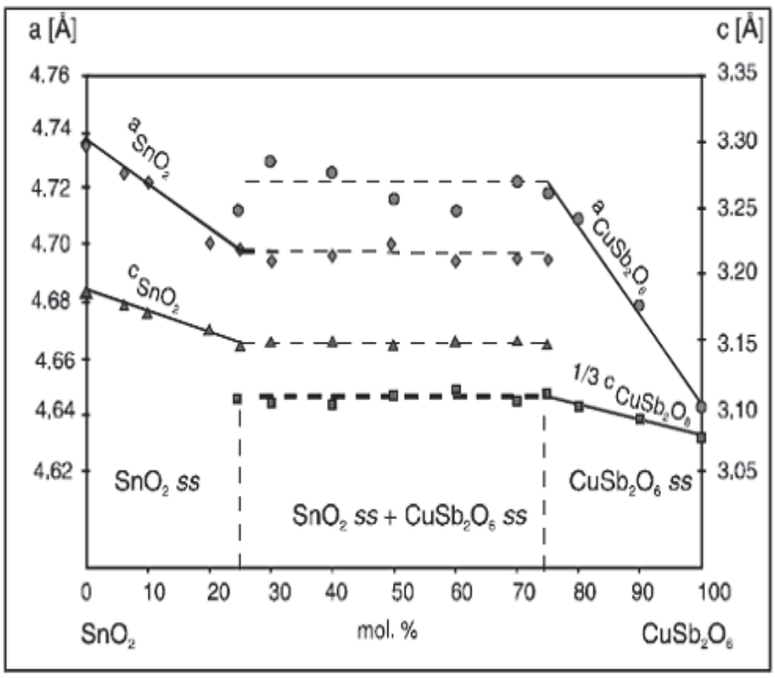

Fig. 9. Variation of the lattice parameters (a, c) for the solid solution SnO_2-$CuSb_2O_6$

Paramagnetic moment values of 1.5, respectively, 1.9 (B.M.) was determinated by Donaldson in the 90-950 K temperature range [Donaldson et al., 1975]. Based upon the cell parameters vs. composition dependence, the solubility limit of SnO_2 in $CuSb_2O_6$ at 1373 K was estimated to be $x_{SnO2} \leq 0.20$. Similarly, for the *trirutile* type solid solution in accordance with Vegard's rule, the lattice parameters varied with the decreasing of SnO_2 content:

$$a_o = 4.679 + 0.0005 \cdot x_{SnO2} \pm 0.002 \text{ Å}$$

$$c_o = 11.065736 + 0.017544 \cdot x_{SnO2} \pm 0.002 \text{ Å}$$

In the case of the $CuSb_2O_6$ solid solution formation, the volume of the unit cell lattice decrease with the decreasing of SnO_2 content. In the same time the β angle value indicates a stabilization of the tetragonal structure of the $CuSb_2O_6$ compound even at room temperature. The magnetic susceptibility($\chi_{g,293K}$) values of about 3.6×10^{-6}cm^3/g obtained for $CuSb_2O_6$ solid solutions was found to lie within the reported limits typical for Cu^{2+} ions It is suggested that the Sn^{4+} incorporation into trirutile lattice take place preferentially on Sb^{5+} sites[Scarlat et al., 2002].

3. Sintered ceramics

For improving properties as thermal and electrical conductivity, translucency and strength it is desirable to eliminate as much of the porosity as possible. For some other application it may be desirable to increase the stregth without decreasing the gas permeability.

The conventional ceramic method, the hot isostatic pressing technique and spark plasma sintering technique are some of the techniques used for the obtaining sintered compacts.
The flow chart of the whole experimental procedure is given in Fig.10.

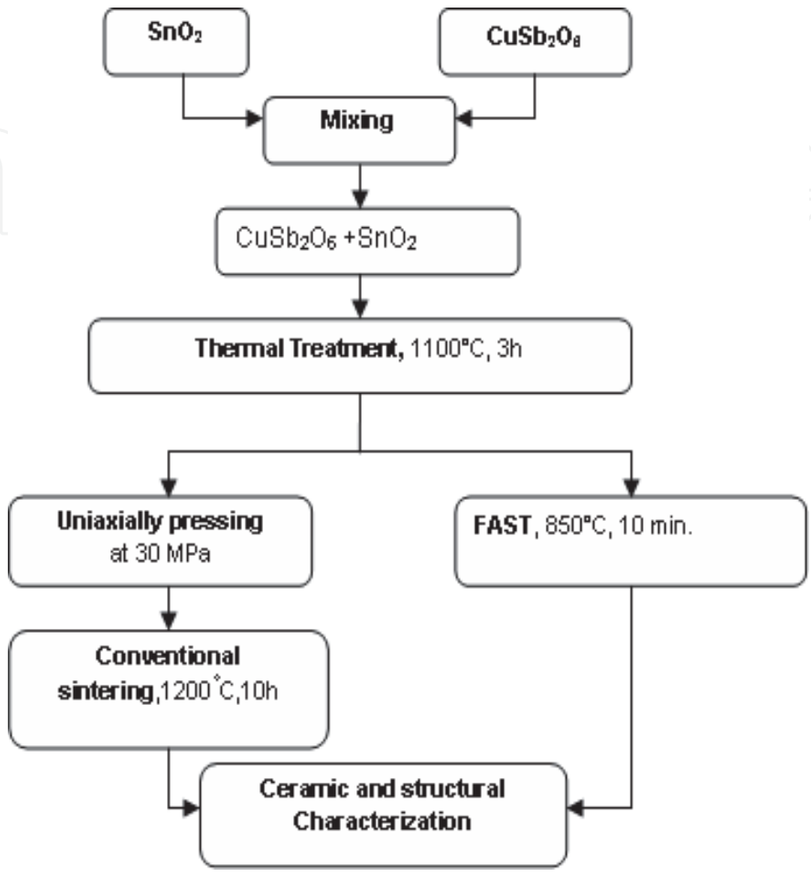

Fig. 10. The flow chart of the whole experimental procedure

3.1 Conventional ceramic method

The usual processing of ceramics, polycrystalline powders are compacted and then thermally treated at temperature sufficient to develop useful properties. During the thermal treatments for the obtaining ceramic compact three major changes commonly occur: (a) an increase in grain size; (b) a change in pore shape; (c) change in pore size and number, usually to give a decreased porosity.
Ceramics belonging to the SnO_2-Sb_2O_3-CuO ternary system thermally treated at lower than 1273K temperatures showed no linear shrinkage but linear dilatation and high porosity pointing out an inadequate sintering[Mihaiu et al., 1999]. The oxide composition that lead to dense ceramics were obtained starting with mixtures with CuO: $Sb_2O_3 \geq 1$ and the SnO_2 content >40 mol% at 1373 K.
Dense ceramics with zero porosity and relative density >94%($d_r = d_{exp}/d_c$).have been reported only in the compositional range with >85mol% SnO_2 and thermal treatment at 1473 K, four hours[Popescu et al.,2002]. For the theoretical density authors [Mihaiu et al., 2005]used the following relation:

$$d_c = \frac{2(1-x)A_{Sn} + 2\frac{x}{3}A_{Cu} + 2\frac{2x}{3}A_{Sb} + 4A_O}{N_A \cdot V_{SnO_{2(ss)}}} \quad (7)$$

in which :A_{Sn}, A_{Cu}, A_{Sb} and A_O are the atomic weights of tin, copper, antimony and oxygen, N_A is Avogadro's number and $V_{SnO2(ss)}$ unit cell volume of the solid solution calculated from the X-ray measured lattice parameters. At 1373 K ceramics formed by the incorporation of the $CuSb_2O_6$ in SnO_2 matrix have not the ability to sinter by conventional sintering method authors [Mihaiu et al., 2005]. Thus, for the $Sn_{0.75}Cu_{0.083}Sb_{0.167}O_2$ composition after thermal treatment three hours, 8.45 % porosity and a relative density of 64.53% have been reported [Mihaiu et al., 2005]. A better sintering capability of the samples with the same compositions was observed from the initial oxides (SnO_2,, CuO and Sb_2O_3) mixtures (72,12% relative density). This difference in the obtained relative density values may be related only to the better sintering capabilities of the sample prepared starting from the initial oxides; as a result of the simultaneously proceeding of the sintering and the formation process of the SnO_2 based solid solution, the latter taking place in stages and thus increasing the whole reactivity of the system. On the other hand, the presence of some un-reacted CuO may develop the formation of a liquid phase at high temperatures. Such a liquid phase rich in CuO was evidenced in the SnO_2–Sb_2O_3–CuO based compositions even for short sintering times[7] and its presence may thus significantly improve the densification properties of the latter sample. The microstructure developed is vizualized by SEM in the Fig.11 (a and b) [Scarlat et al., 2003]

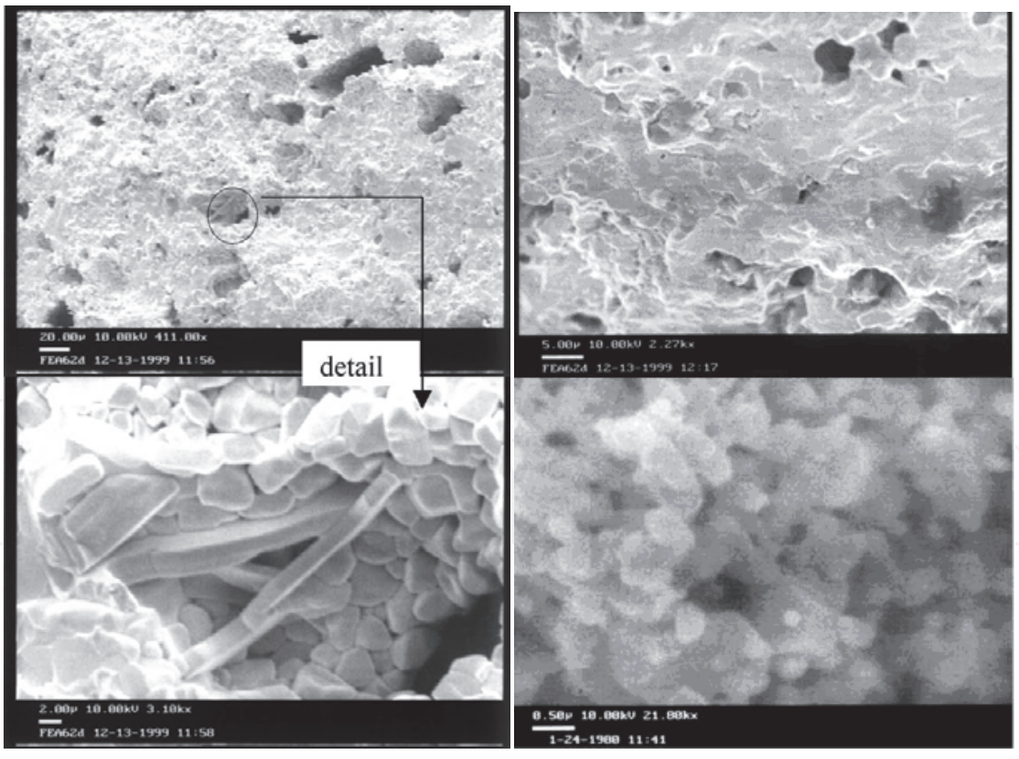

a) b)

a) starting with ternary mixture of 80 mol% of SnO_2, 10 mol% of Sb_2O_3 and 10 mol% of CuO
b) starting with binary mixture 90 mol% of SnO_2 and 10 mol% of $CuSb_2O_6$

Fig. 11. SEM micrographs of the sintered $Sn_{0.75}Cu_{0.083}Sb_{0.167}O_2$ composition at 1373 K, 3 hours

The presence of grains of about the same shape and size with some local and occasional inhomogeneties and a high amount of voids are evidenced.
The SEM images of the $Sn_{0.75}Cu_{0.083}Sb_{0.167}O_2$ composition (binary mixtures) thermally treated at 1373 K , ten hours and at 1473 K three hour are presented in Fig.12(a and b). By prolonged thermal treatment the sintering process is enhanced, but some pores (about 0.5 μm) are still enclosed in the obtained dense ceramics (Fig. 12. a). For the sample Thermally treated at 1473 K (Fig.12 b) the presence both of the primary phase composed of the relative uniform grains with the sizes more of 10 μ, and of the secondary phase with smaller size grains can be observed. However, the supplementary addition of CuO to the $Sn_{1-x}Cu_{x/3}$ $Sb_{2x/3}O_2$ solid solutions did not improve essentially the sintering abilities of the sample [Mihaiu et al., 2003]

3.2 Spark plasma sintering technique(SPS)

The spark plasma sintering technique (SPS) is a nonconventional densification method, which has been succesfully applied to dificult-to-sinter materals. A pulsed low-voltage high current is applied to loose powder loaded into a graphite punch and die unit. The pulsed current promotes electrical discharges at powder particle surfaces, thus activating them for subsequent bonding. A modest pressure (<100MPa) is applied throughout the sintering cycle. Densities in excess of 99% have been reported by SPS sintering of ceramics powders, such as AlN, Al_2TiO_5 or TiN without any sintering additives [Scarlat et al., 2003].

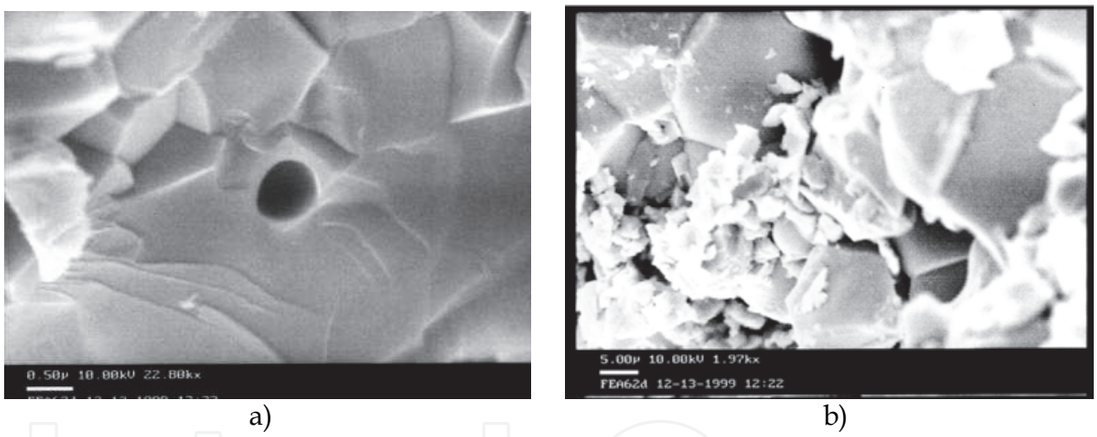

a) b)

Fig. 12. SEM micrographs of the sintered $Sn_{0.75}Cu_{0.083}Sb_{0.167}O_2$ composition starting with binary mixture 90 mol% of SnO_2 and 10 mol% of $CuSb_2O_6$: a) thermally treated at at 1373 K, 10 hours ; and thermally treated at at 1473 K, 3 hours.

The sintering modulus of the SPS machine is presented in Fig.13.
The solid solutions of the $Sn_{0.82}Sb_{0.18}O_2$ composition (prepared after thermal treatment at 1273 K, 3 hour of the tin and antimony oxide mixture) and of $Sn0_{0.75}CuO_{0.083}Sb_{0.167}O_2$ composition have been densified by Spark plasma sintering technique. The sintered compacts with high relative density of 92.44% in the case of $Sn_{0.82}Sb_{0.18}O_2$ composition and 99.6% for $Sn_{0.75}$ $Cu_{0.083}$ $Sb_{0.167}O_2$ composition have been reported by [Scarlat et al., 2003; Mihaiu et al.,2005]. The SEM photographs of the samples $Sn_{0.82}Sb_{0.18}O_2$ and $Sn_{0.75}Cu_{0.083}Sb_{0.167}O_2$ illustrated in Figs.13 (a and b) indicate the obtaining of the consolidated microstructure with the grain sizes lower than 1μ. However, the very fine homogeneous grains of the sample $Sn_{0.82}Sb_{0.18}O_2$ in comparison with the sample $Sn_{0.75}Cu_{0.083}Sb_{0.167}O_2$ could be notice.

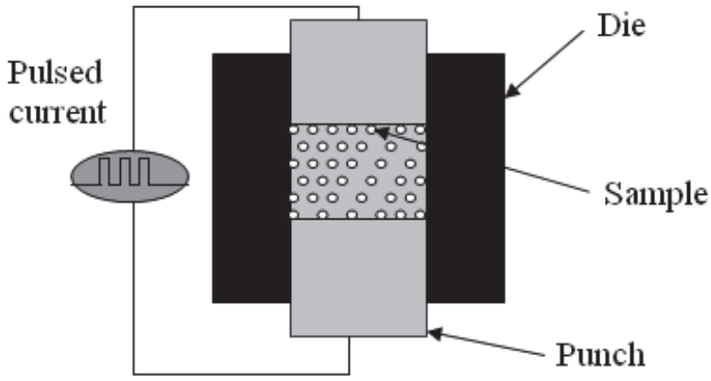

Fig. 13. Sintering modulus of the SPS machine

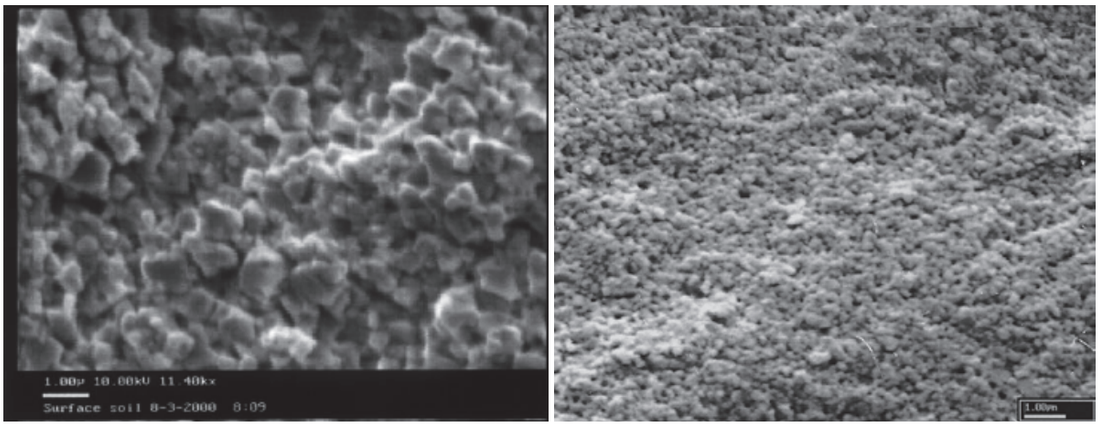

a.) b.)

Fig. 14. SEM micrograph of the compats sintered by Spark plasma sintering technique (SPS): a.) solid solution of $Sn_{0.75}Cu_{0.083}Sb_{0.167}O_2$ composition obtained after thermal treatement at 1373 K , 3 hours[Scarlat et al.,2004]; b.) solid solution of $Sn_{0.82}Sb_{0.18}O_2$ composition obtained after thermal treatement at 1273 K , 3 hours [Scarlat et al., 2003]

Even though the exact mechanism of the enhanced SPS densification is not yet known, it is assumed that the pulsed electrical current creates favorable conditions for the removal of impurities and activation of powder particle surfaces. Some arcing or electrical discharge phenomena at particle- to-particle contacts may be responsible for adsorbate elimination or surface ''cleaning'', thus creating favorable conditions for subsequent particle bonding. This activation explained the high densities obtained in ceramics without additives and direct grain-to-grain contact at atom scale observed by HREM in ceramics and metals. In addition to the little coarsening due to a very short time at high temperatures, the final nanometer grain sizes by SPS sintering also reflect a minimal coarsening during the heating up stage.

4. Electrical behaviour of the SnO_2-based ceramics

The electrical behaviour of the dense ceramic masses in the system was approached a in Sn-Sb-Cu-O papers [Zuca et al., 1995, 1999; Mihaiu et al., 200; ,Scarlat et al., 2003, 2004; Popescu

et al., 2002] Electrical conductivity measurements were effected in the 77-1100 K temperature range on two types of materials with distinct structure:

- SnO_2 monophasic ceramics with rutile type structure
- ceramics consisting of phase mixtures: SnO_2 +$Cu_4SbO_{4.5}$ or

$$SnO_2 + Cu_4SbO_{4.5} + Cu\ Sb_2O_6$$

Measurements in the 300-1100 K temperature range were accomplished in the cell presented in Fig.15

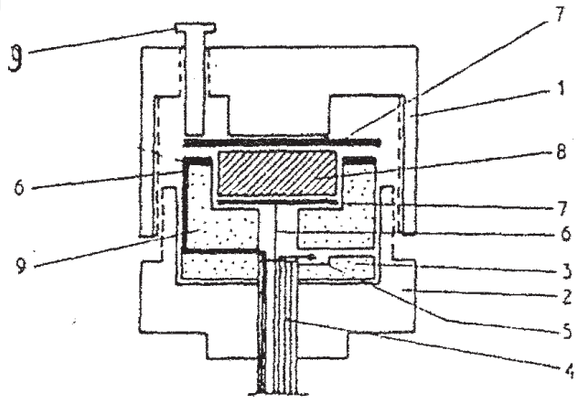

1, 2 refractory steel threated bodies; 3 boron nitride ring; 4 four channel insulator; 5 Pt-PtRh thermocouple; 6 platinum wire; 7 platinum electrodes; 8 semiconductor pellet; 9 boron nitride support; 10 stainless steel screw; 11 platinum ring.

Fig. 15.The pellet holder for conductivity measurements.

An other serie of measurements were realized in the low temperature range between 77-300 K .The dependence of the resistivity on the temperature and the values of Seebeck coefficient for some selected samples is shown in Fig. 16(a) and Tables 4. A small variation of the samples consisting of SnO_2 ss with the temperature was found. The samples consisting of phase mixtures show an important decrease of three orders of magnitude of the resistivity up to 800K. Over this temperature, all the samples have a similar behaviour.
A graphical analysis of the linear of ln k vs.1/T dependence in the two temperature ranges studied(Fig. 16. b) brings about new additional information. According to these data all samples exhibit a n-extrinsic conductivity whose activation energy ranges within 0.04-0.3 eV. As it could be seen in Fig.16 (b-inserted) for the samples composed from a unique phase single Arrhenius line was obtained over the whole 300-1100 K, similar behavoiur of the sample where Sb_2O_3 and CuO act as dopant [Zuca et al., 1991]. However some distinctive tendencies were recorded in Fig.17 for samples consisting of a mixture of phases. As seen a marked change of slope takes place at temperatures exceeding 600K which suggests a possible modification of charge carriers involved in conduction process. Indeed Shimada and Mackenzie identified in the temperature range under discussion, the following chemical reaction [Shimada & Mackenzie, 1982]:

$$Cu_4SbO_{4.5} \leftrightarrow CuSb_2O_6 \quad (8)$$

Sample	Oxide composition			Phase Composition	Seebeck Coeficient (μV/K)
	SnO_2	Sb_2O_3	CuO		
t_1	95	1	4	SnO_{2ss}	-1.7
A_1	80	10	10	SnO_{2ss}	-1.6
A_2	60	20	20	SnO_{2ss}	-1.7
B_3	50	10	40	$SnO_{2ss}+Cu_4SbO_{4.5}$	-
B_4	50	20	30	SnO_{2ss}	-3
B_5	40	20	40	SnO_{2ss}	-1.8
B_9	30	10	60	$SnO_{2ss}+Cu_4SbO_{4.5}$	+10
B_{10}	20	30	50	$CuSb_2O_6$+ SnO_2 $+Cu_4SbO_{4.5}$	-

Table 4. Oxide composition and phase composition

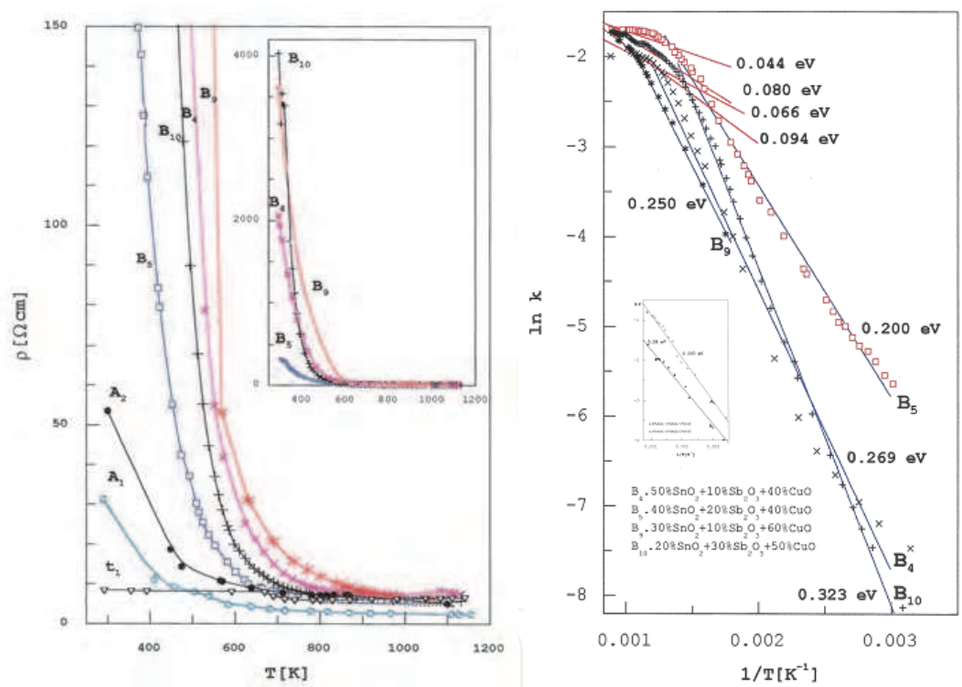

a) b)

Fig. 16. Electrical behavior: a) Dependence ρ plotted against temperature; b) Arrhenius behaviour in 300-1100K temperature range for various samples; solid solutions of $Sn_{0.75}Sb_{0.17}Cu_{0.08}O_2$ and $Sn_{0.5}Sb_{0.33}Cu_{0.17}O_2$ composition are inserted in b.)

Which could generate the behaviour shown in Fig17.b By an additional incorporation of $CuSb_2O_6$in the SnO_2 labilized lattice with increasing temperature[Zuca et al., 1999] The small negative values ofthe Seebeck coeficient confirm the electronic conduction in all samples except the sample which consists of a phase mixture. În this case the existence of Cu4SbO4.5 compound even at 300K temperature can favour a different mechanism of carrier motion (a possible p-type conductivity), which accounts for the Seebeck coefficient which take comparatively high positive value.

5. Conclusions

Discussion on the high-temperature interactions of components in the binary SnO_2-Sb_2O_3, SnO_2-CuO, Sb_2O_3-CuO, SnO_2-$CuSb_2O_6$ systems and in the ternary SnO_2-Sb_2O_3-CuO system was presented. The complexity of phase formation and phase composition evolution with thermal treatment temperature was established.

Results on the sintering capacity and consequently the densification using coventional and spark plasama sintering were presented. The powders sintering behavior depends on the method used. Highly densified ceramics were obtained only by using SPS sintering.

According to the electrical data all samples exhibit n-extrinsic conductivity whose activation energy ranges within 0.04-0.3 eV.

6. References

Bueno, P. R. Varela, J.A. & Longo, E. (2007). Admittance and dielectric spectroscopy of polycrystalline semiconductors *J. Eur. Ceram. Soc.* 27 : 4313–4320

Caldararu, M.. Mihaiu, S. Spranceana, D. Zaharescu, M. Popa, V.T. & Ionescu, N.I. (1999). The role of Hydration-dehydration effects on oxygen adsorption on SnO_2. *R ev.Ruom. Chim*. 44 (11-12) : 1115-1121

Chadwick, A.V. (1993). EXAFS studies of dopant sites in metal oxides. *Solid State Ion*. 63–65: 721-726

Dolet, N. Heintz, J. M. Onillon, M. & Bonet, J. P. (1992). Densification of 0.99SnO2–0.01CuO Mixture: Evidence for Liquid Phase Sintering, *J. Eur. Ceram.Soc.*, 9: 19–25

Heintz, J. M. Rabardel, L. Onillon, M. & Bonnet, J. P. (1995). Sintering Mechanisms of 0.99SnO2–0.01CuO Mixtures. *J. Mater. Sci.*, 30 (2): 365–368

Donaldson J. D. Kjekshus, A. Nicholson, D. G.& Rakke, T. (1975). Properties of Sb-compounds with Rutile –like Structures *Acta Chem.Scan.* A29,: 803

Dusastre, V. &Williams, D.E. (1998). Sb(III) as active sites for water adsorption on Sn(Sb)O2, and its effect on catalytic activity and sensor behavior *J. Phys. Chem.* B 102: 6732-6738

Harrison, P.G. Bailey, C.& Azelee, W. (1999). Modified tin(IV) oxide (M/SnO2 M = Cr, LA, Pr, Nd,Sm, Gd) catalysts for oxidation of carbon monoxide and propane. *J. Catal*. 186: 147-151

Kikuchi, T. Watanabe, A. & Uchida. K. (1983). Formation of rutile type solid solutions in Pseudobinary Systems SnO_2-ABO_4 (A=Ga, Cr; B= Nb, Ta, Sb^{5+}) and SnO_2- AB_2O_6 (A=Mg, Zn; B= Sb^{5+}) *Yogyo-Kyokai Shi* 91(3): 110-116

Mihaiu, S. Zaharescu. M., Crişan D., & Zuca, Şt.. (1995). Stucture and Properties of the Solid Solutions in the Sn-Sb-Cu-O System" *Adv.Sci.&Technol.,B3*(Ceramics Charting the Future), pp. 702-710

Mihaiu, S. Scarlat, O. Radovici, C. & Zaharescu M. (2000). Phase Formation Sintering in the SnO_2- $CuSb_2O_6$ Pseudobinary System"Powder Metallurgy Science and Technology, *Proceedings of Second International Conference on Powder Metallurgy RoPM* . Ed. G. Arghir, U.T.Pres, Cluj-Napoca, 1, pp. 73-77

Stanica N. & Zaharescu M. (2001). Oxide Materials with Magnetic Properties in the SnO_2-$CuSb_2O_6$ Pseudobinary System. *J. Optoelect. Adv. Mater.* 3: pp. 913-918

Mihaiu, S. Scarlat O. Aldica Gh.& Zaharescu M. (2001). SnO_2 Electroceramics with Various Additives *J. Eur.Ceram. Society*, 21: pp. 1801-180

Mihaiu, S. Dragan, N. Scarlat, O.; Szatvanyi, A. Crisan, D. & Zaharescu, M. (2002). Structural Characterisation of the SnO_2Ceramics with Various Additives *Rev. Roum. Chim.* 47(9) : pp. 843-849

Mihaiu, S. Scarlat , O. Aldica, Gh. & Zaharescu M. (2003). Electronic Conduction of the $Sn_{1-x}Cu_{x/3}Sb_{2x/3}O_2$ (x<1/2) Rutile Type Structures. *J. Optoelectr. Adv. Mat.*, 5,:913-918

Nakua, A. Yun, H. Reimers, J. N. Greedan, J. E. & Stager, C. V. (1991). Crystal Structure, Short Range and Long Range Magnetic Ordering in Cu Sb_2O_6 . *J. Solid State Chem* 91: 105-110

Orel, U. Stangar, L. Opara, U. Gaberscek, M. & Kalcher, K. (1995). Preparation and Characterization of Mo- and Sb:Mo-Doped SnO2 Sol–Gel-Derived Films for Counterelectrode Applications in Electrochromic Devices. *J. Mater. Chem.*, 5 (4): 617–624

Park, P.W. Kung, H.H. Kim, D.-W. & Kung, M.C. (1999). Characterization of SnO2/Al2O3 lean NOx catalysts. *J. Catal.* 184: 440-446

Presley, R.E. Munsee, C.L. Park, C.-H. Hong, D.J. Wager, F. & Keszler D.A. (2004). Tin oxide transparent thin-film transistors, *J. Phys. D* 37: 281-287

Popescu, A.M. Mihaiu, S. & Zuca, S. (2002). Microstructure and Electrochemical Behaviour of Some SnO_2-Based Inert Electrodes in Aluminium Electrolysis", *Z.Naturforsch.* 57 a: 71-75

Popescu, A.M. Mihaiu, S. Constantin V.& Zaharescu M. (2007). Processing of oxide advanced ceramics as inert electrodes. *J. Optoelect. Adv.Mater.* 9(7): 2227- 2231

Rockenberger, J. Felde.U. Tischer, M. Troger, L. Haase, M. & Weller, H. (2000). Near edge X-ray absorption fine structure measurements (XANES) and extended X-ray absorption fine structure measurements (EXAFS) of the valence state and coordination of antimony in doped nanocrystalline SnO_2, *J. Chem. Phys*.112: 4296 Scarlat, O. Mihaiu, S.M. & Zaharescu M.(1999). CAS'99 *Proceedings of International Semiconductor Conference*, 22nd Edition, October 5 - 9, Sinaia, Romania., 1: 401

Scarlat, O. Mihaiu, S.& Zaharescu M (2002). Subsolidus Phase Relations in the SnO_2 - $CuSb_2O_6$Binary System". *J Eur Ceram Soc.*, 22: 1839-1846

Scarlat, O. Payne, A.C. Mihaiu, S. Aldica, Gh. & Zaharescu, M. (2003). A Study of the SnO_2 and $CuSb_2O_6$ Based Solid Solutions: Electrical and Magnetic Properties. *J. Optoelectr. Adv. Mat.*, 5: 997-1002

Scarlat, O. Mihaiu, S. Aldica, Gh. Zaharescu, M. & Groza, J. R. (2003). Enhanced Properties of Tin (IV) Oxide Based Materials by Field-Activated Sintering. *J.Am. Ceram. Soc.* 86: 893- 897

Scarlat, O. Mihaiu, S. Aldica Gh., Groza, J. & Zaharescu, M. (2004). Semiconducting Densified SnO_2- Ceramics Obtained by a Novel Sintering Tehnique. *J. Eur. Ceram. Soc.* 24 : 1049-1052

Slater, B. Catlow, C.R. Gay, D.H. Williams, D.E. & Dusastre, V. (1999). Study of surface segregation of antimony on SnO2 surfaces by computer simulation techniques. *J. Phys. Chem. B* .103: 10644.

Stan, M. Mihaiu, S. Crisan, D. & Zaharescu, M. (1997). Subsolidus Equilibriq in the Sn-Sb-Cu-O System. *Key Engineering Materials*, Ed. Trans. Tech. Publications, Switzerland. p.790 -793

Stan, M. Mihaiu, S. Crisan, D. & Zaharescu, M. (1998). Subsolidus Equilibria in the Sb-Cu-O System. *E. J. Solid State Inorg.Chem* .35: 243-254

Varela, O. J. Whittemore, & M. J. Ball, (1990). Pore Size Evolution during Sintering of Ceramic Oxides. *Ceram. Int.*, 16: 177–189

Varela, O. J. Gouvea, D. Longo, E. Dolet, N. Onillon, M. & Bonnet, J. P. (1992). The Effect of Additives on the Sintering of Tin Oxide. *Solid State Phenom.*, **25** (26): 259–268

Vlasova, M. V. Dıˆsel, D. E. & Kakazei N. G. (1990). Protzesı Formirovania Dispernıh Chastitz pri Termincheskoi Ogragotke Smesei Ghidroksidov Olova i Surımı. *Neorg.Mater.*, 26 (7): 1486–1490

Volta, J.C. Benaichouba, B. Mutin,I. & Vedrine, J.C (1983). Comparative study of SnSbO and SnSbFeO mixed oxide catalysts in propene mild oxidation. Physico-chemical And catalytic investigation. Appl.Catal. 8: 215-236

Wagner, F. (2003). Transparent electronics. *Science* 300: 1245.

Wyckoff, R.W.G. (1963). Crystal Structures, vol.I-II, Ed. John Wiley & Sons, New York, London, Sidney,1964

Zaharescu, M. Mihaiu, S. Zuca, S. & Matiasovsky, K. (1991). Contribution to the study of SnO_2 -based ceramics.I.High- temperature interaction of tin (IV) oxide with antimony(III) oxide and copper(II) oxide. *J.Mat.Sci.* 26: 1666-1672

Zaharescu, M. Mihaiu**,** S. Crişan, D.& Zuca, Şt (1993). Structure and properties of ceramics in the SnO_2- Sb_2O_3-CuO system.. *The Proceedings of the European Ceramic Society Conference (THIRD ECerS)* Third Euro-Ceramics (Eds. P.Duran and J.F.Fernandez), Faenza Editrice Iberica S.L., Spain, 2: 359-364

Zaharescu, M. Mihaiu, M.S. & Zuca S (1999). Ceramic Properties of the Sintered Materials in the Sn-Sb-Cu-O System. *Advance Science and Technology of Sintering*, Ed.Kluwer Academic/Plen. Publis., N.Y. 251-258.

Zuca, S. Terzi, M. Zaharescu, M. & Matiasovsky ,K. M. (1991). Contribution to the study of SnO2- based ceramics: Part II. Efect of various oxide additives on the sintering capacity and electrical conductivity of SnO2. *J. Mater. Sci*. 26:1673-1676

Zuca, S. Mihaiu, S**.** & .Zaharescu M. (1995). Electrical Properties of the Ceramics în the Sn-Sb-Cu-O System. *Electroceramics,* Ed. Gusmano G. , Traversa E.,5: 373-380

Zuca, S. Aldica, Gh.; Mihaiu, M.S. Zaharescu, M. (1999). Electrical Behaviour vs Temperature of the Ceramics in the Sn-Sb-Cu-O System" Advances in Science and Technology. 13, Ceramics: Getting into the 2000's, Part B, Edited by P.Vincenzini, Italy, TECHNA, Faenza: p.345-352

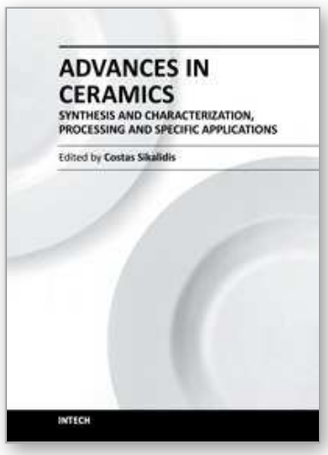

Advances in Ceramics - Synthesis and Characterization, Processing and Specific Applications

Edited by Prof. Costas Sikalidis

ISBN 978-953-307-505-1
Hard cover, 520 pages
Publisher InTech
Published online 09, August, 2011
Published in print edition August, 2011

The current book contains twenty-two chapters and is divided into three sections. Section I consists of nine chapters which discuss synthesis through innovative as well as modified conventional techniques of certain advanced ceramics (e.g. target materials, high strength porous ceramics, optical and thermo-luminescent ceramics, ceramic powders and fibers) and their characterization using a combination of well known and advanced techniques. Section II is also composed of nine chapters, which are dealing with the aqueous processing of nitride ceramics, the shape and size optimization of ceramic components through design methodologies and manufacturing technologies, the sinterability and properties of ZnNb oxide ceramics, the grinding optimization, the redox behaviour of ceria based and related materials, the alloy reinforcement by ceramic particles addition, the sintering study through dihedral surface angle using AFM and the surface modification and properties induced by a laser beam in pressings of ceramic powders. Section III includes four chapters which are dealing with the deposition of ceramic powders for oxide fuel cells preparation, the perovskite type ceramics for solid fuel cells, the ceramics for laser applications and fabrication and the characterization and modeling of protonic ceramics.

InTech Europe
University Campus STeP Ri
Slavka Krautzeka 83/A
51000 Rijeka, Croatia
Phone: +385 (51) 770 447
Fax: +385 (51) 686 166
www.intechopen.com

InTech China
Unit 405, Office Block, Hotel Equatorial Shanghai
No.65, Yan An Road (West), Shanghai, 200040, China
中国上海市延安西路65号上海国际贵都大饭店办公楼405单元
Phone: +86-21-62489820
Fax: +86-21-62489821

IntechOpen